Dislocation Content Measured via 3D HR-EBSD Near a Grain Boundary in an AlCu Oligocrystal

Timothy Ruggles[1], Jacob Hochhalter[2], Eric Homer[3]
[1]National Institute of Aerospace, [2]NASA Langley Research Center, [3]Brigham Young University

Introduction

Interactions between dislocations and grain boundaries are poorly understood and crucial to mesoscale plasticity modeling. Much of our understanding of dislocation-grain boundary interaction comes from atomistic simulations and TEM studies, both of which are extremely limited in scale. High angular resolution EBSD-based continuum dislocation microscopy provides a way of measuring dislocation activity at length scales and accuracies relevant to crystal plasticity, but it is limited as a two-dimensional technique, meaning the character of the grain boundary and the complete dislocation activity is difficult to recover. However, the commercialization of plasma FIB dualbeam microscopes have made 3D EBSD studies all the more feasible. The objective of this work is to apply high angular resolution cross correlation EBSD to a 3D EBSD data set collected by serial sectioning in a FIB to characterize dislocation interaction with a grain boundary.

HR-EBSD

High angular resolution EBSD (HR-EBSD) is a method of post processing collected EBSD patterns to extract higher levels of detail. Shifts between regions of interest (ROIs) on two patterns are calculated using cross correlation, which may then be related to the relative distortion between the two patterns with a high degree of accuracy. While conventional EBSD has an accuracy of around a quarter degree under ideal circumstances, HR-EBSD is accurate to within approximately 0.006°.

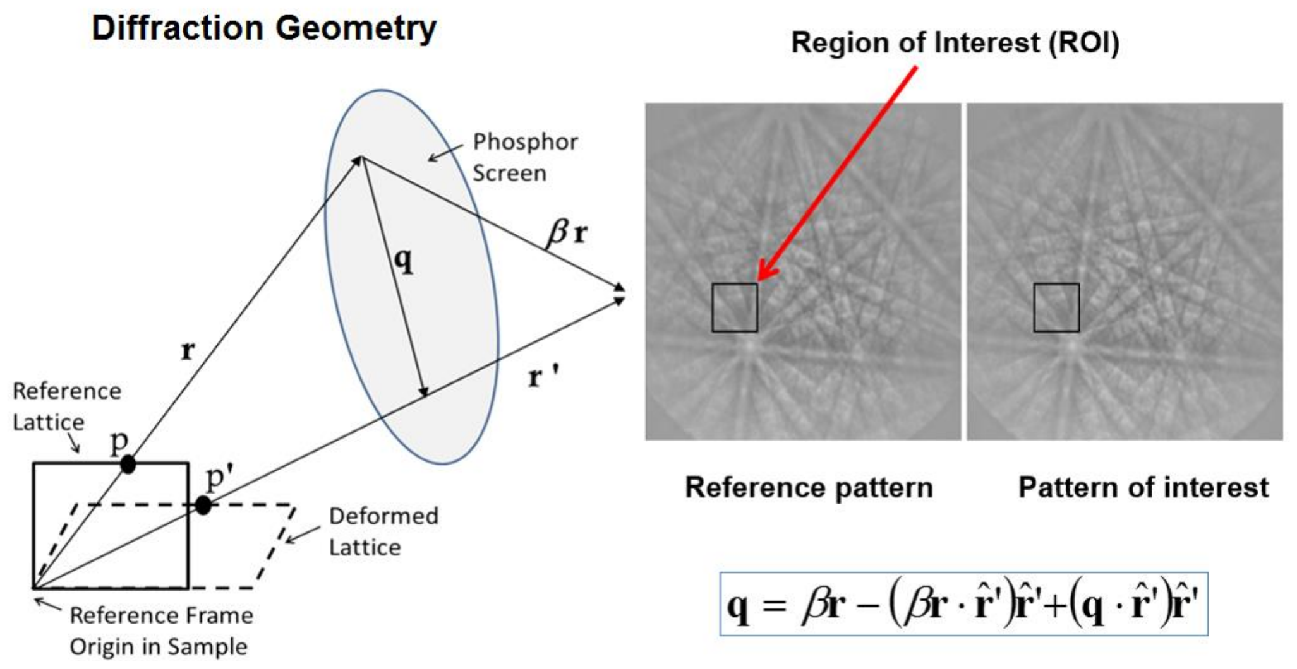

$$\mathbf{q} = \beta\mathbf{r} - (\beta\mathbf{r}\cdot\hat{\mathbf{r}}')\hat{\mathbf{r}}' + (\mathbf{q}\cdot\hat{\mathbf{r}}')\hat{\mathbf{r}}'$$

Fig. 1 – Illustration of high angular resolution EBSD.

This precise measure of distortion may be used to numerically determine Nye's tensor:

$$\alpha = \nabla \times \beta$$

Nye's tensor may then be related to the dislocation content of each individual dislocation type using the following minimization:

$$\underset{\rho^t}{\text{minimize}}\ f = \sum_{t=1}^{N} \left| w^t \rho^t \right| \quad \text{s.t.} \quad \alpha_{ij} = \sum_{t=1}^{N} \rho^t b_i^t v_j^t$$

Note that Nye's tensor may be approximated using conventional EBSD with lower resolution. In 2D EBSD dislocation microscopy, HR-EBSD has supplanted this approximation, but it is still prevalent in 3D EBSD dislocation microscopy due to the difficulty of aligning the serial sections for HR-EBSD.

Material and Microscopy

An AlCu (6% Cu) copper oligocrystal was used for this study. The sample was precipitation hardened and deformed to 11% elongation as measured by digital image correlation. A grain boundary with a high degree of dislocation activity was selected. Due to its curvature, the grain boundary character is highly variable along the boundary.

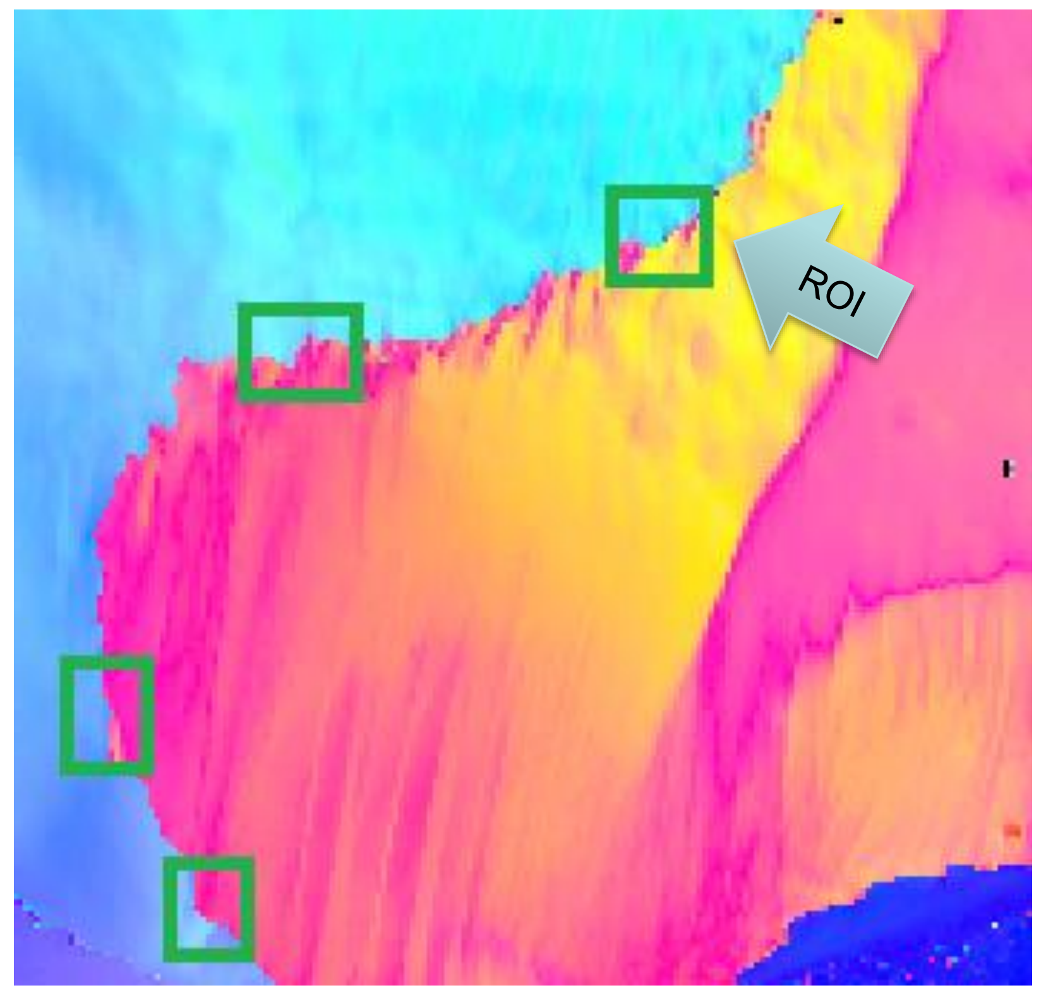

Fig. 2 – Inverse pole figure of the grain boundary of interest. The area selected for 3D analysis is highlighted, as well as possible future ROIs.

A smaller ROI was selected along the grain boundary for 3D study. The 3D analysis was performed in an FEI Helios^{TM} Plasma FIB DualBeam. The ROI was lifted out in a block and then scanned and sectioned to produce four slices of EBSD data. The area examined was approximately 50x40 microns and the step size of the EBSD raster (and the slice thickness) was 200 nm. The entire analysis took about a day, most of which was EBSD acquisition.

Slice 1: 0-50 nm depth

Slice 2: 200 nm depth

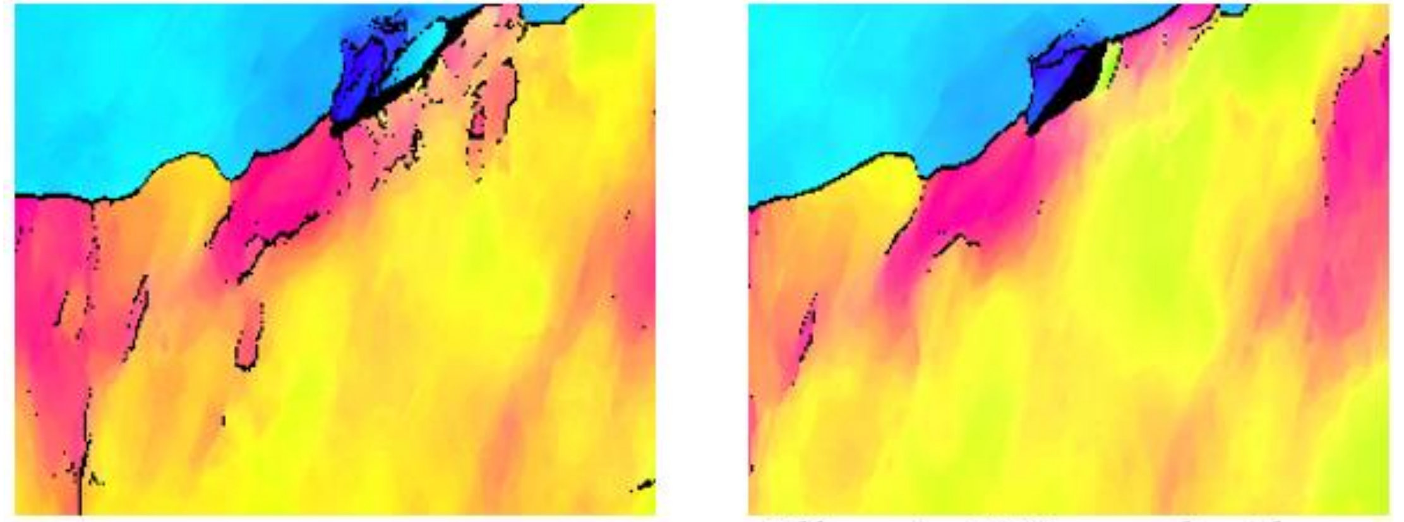

Slice 3: 400 nm depth

Slice 4: 600 nm depth

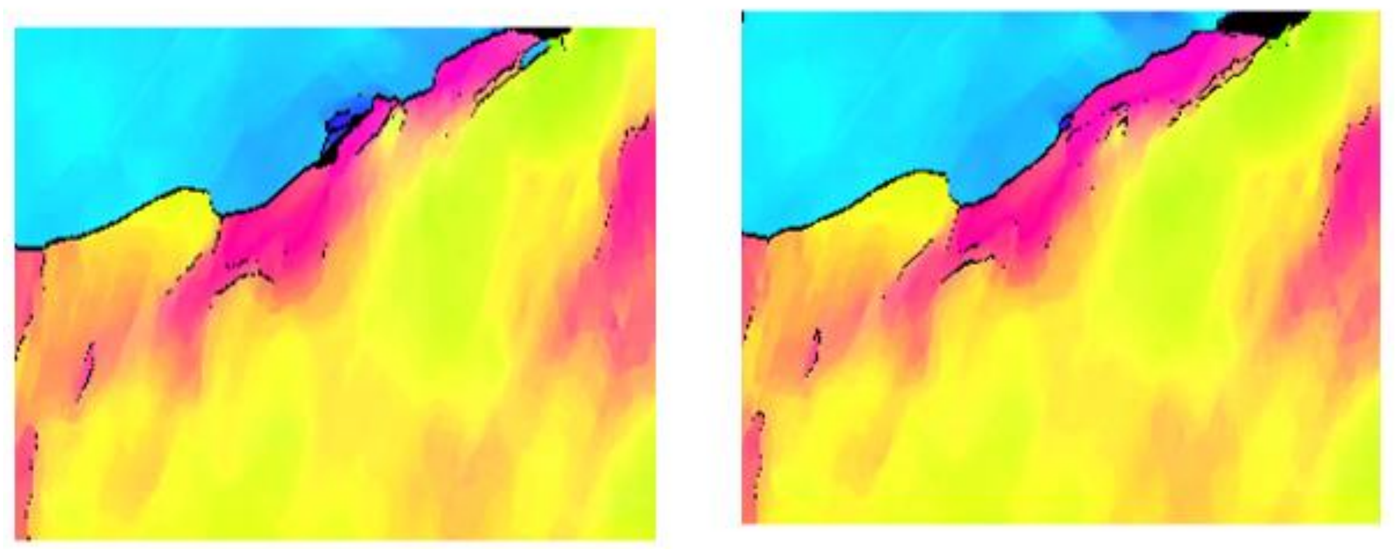

Fig. 3 – Invers pole figure of each slice of the examined region. Each scan is 50x40 microns

Alignment

Efforts to align the layers using a physical feature (the edge of the block) were unsatisfactory. Instead, the slices were aligned to the nearest pixel by minimizing the average misorientation between corresponding points of each slice, as in Konijnenberg, et al., 2015*. The resulting measured distortion gradient was calculated.

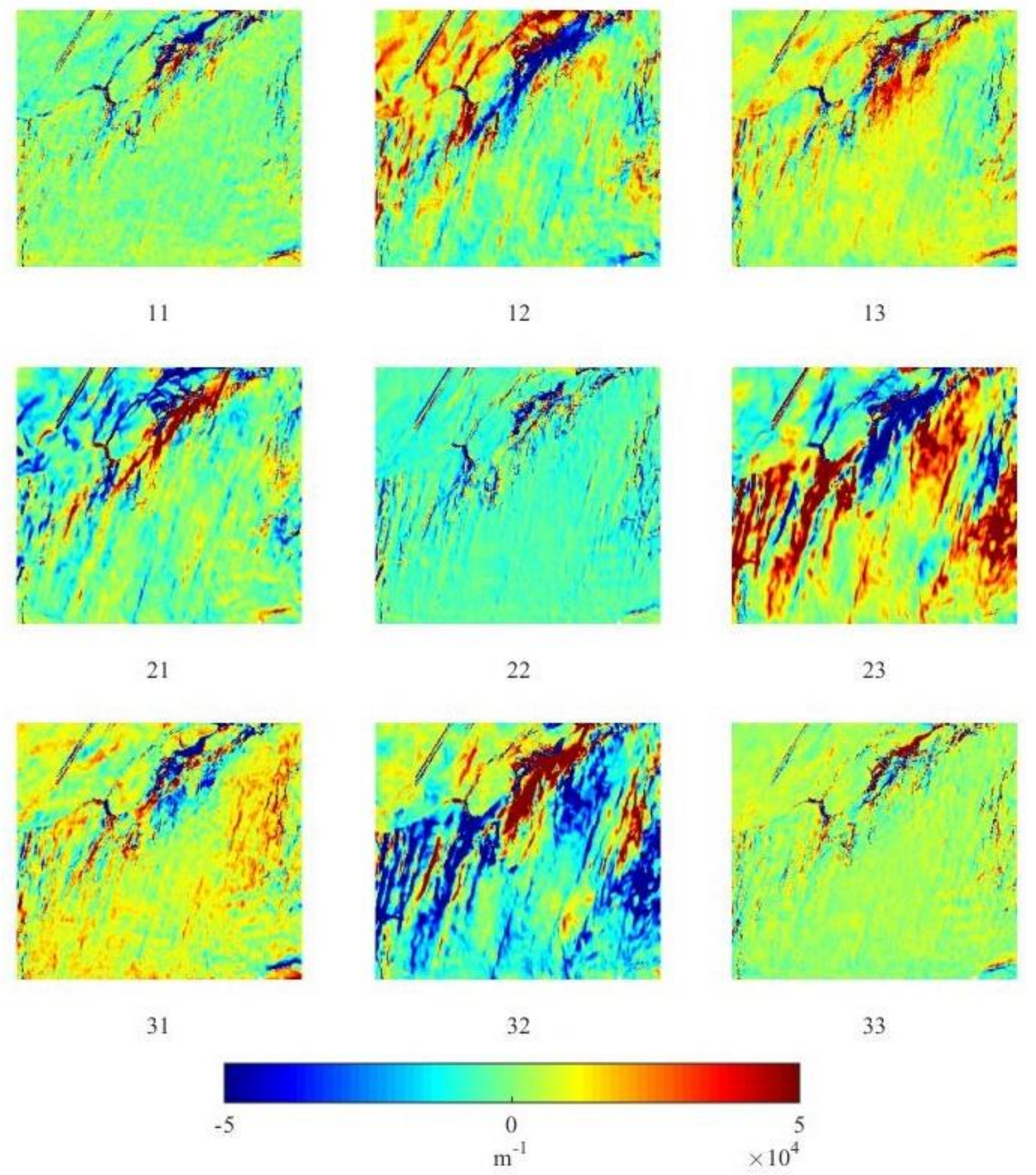

Fig. 4 – Derivative normal to the sample surface for all nine distortion components on slice 3.

Grain Boundary Character

Once the shifts were determined, individual ROIs along a section of the grain boundary were cross correlated between slices to reconstruct the three dimensional shape of the grain boundary.

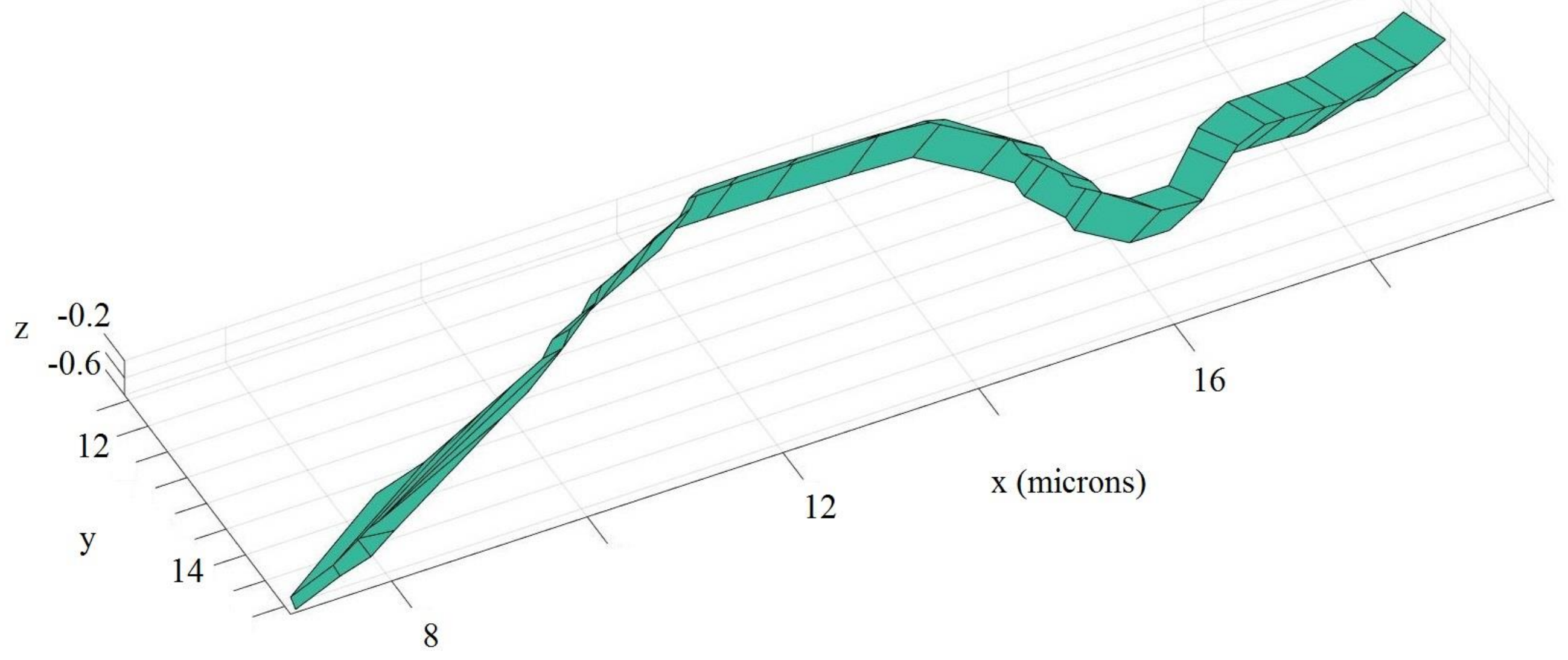

Fig. 5 – Model of the grain boundary, generated via cross correlation.

*P. Konijnenberg, S. Zaefferer, D. Raabe, Assessment of geometrically necessary dislocation levels derived by 3D EBSD, Acta Materialia 99 (2015) 402 – 414.

Results

Distortion gradients and dislocation content were calculated using a modified version of OpenXY, an open source HR-EBSD code available on GitHub. The total dislocation content is about 3.52 times higher with the inclusion of the out of plane distortion derivative, much higher than expected, suggesting that there are still significant alignment issues.

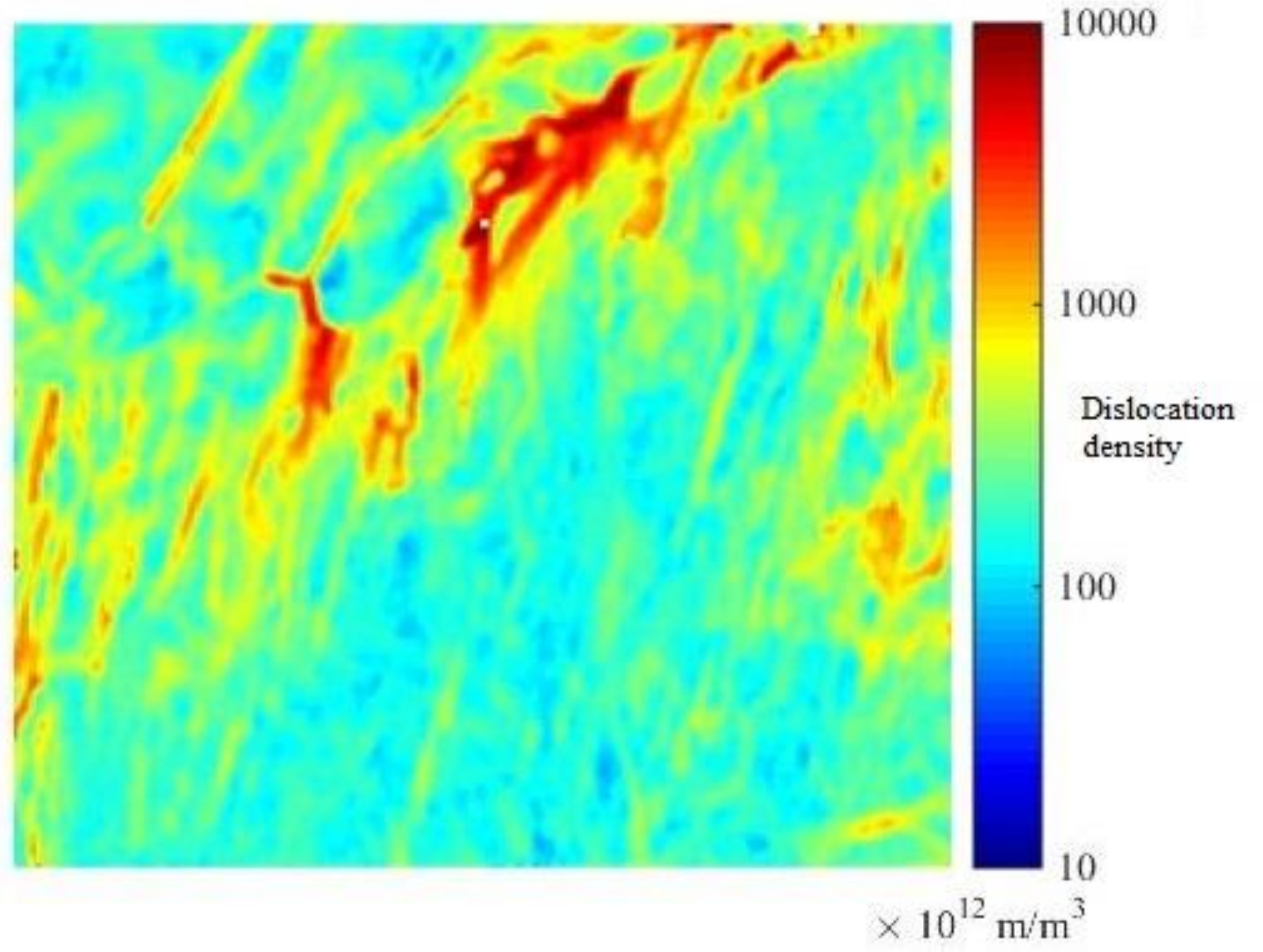

Fig. 6 – Total dislocation density when derivatives normal to the surface are included on slice 3.

Conclusions and Future Work

- Three dimensional high angular resolution cross correlation EBSD analysis was applied to an AlCu oligocrystal to measure dislocation densities around a grain boundary.
- Distortion derivatives associated with the plasma FIB serial sectioning were higher than expected, possibly due to geometric uncertainty between layers.
- Future work will focus on mitigating the geometric uncertainty and examining more regions of interest along the grain boundary to glean information on dislocation-grain boundary interaction.

Acknowledgments

The microscopy work for this study was performed and facilitated by collaborators at FEI, Barlomiej Winiarski, Tim Burnett, Ron Kelley and Bryan Majkrzak.

Further Information

For questions or comments please feel free to contact:
Timothy Ruggles– timothy.ruggles@nasa.gov

For further information on EBSD dislocation microscopy, see:
T. Ruggles, D. Fullwood, J. Kysar, Resolving geometrically necessary dislocation density onto individual dislocation types using EBSD-based continuum dislocation microscopy, International Journal of Plasticity 76 (2016) 231 – 243.